

Fermi National Accelerator Laboratory

FERMILAB-Conf-94/317-E

Electroweak Physics from the Tevatron

Larry Nodulman

*Fermi National Accelerator Laboratory
P.O. Box 500, Batavia, Illinois 60510*

*HEP Division, Argonne National Laboratory,
Argonne, Illinois 60439*

September 1994

*For Proceedings of the Conference on Radiative Corrections: Status and Outlook,
Gatlinburg, TN. June 27 - July 1, 1994*

Disclaimer

This report was prepared as an account of work sponsored by an agency of the United States Government. Neither the United States Government nor any agency thereof, nor any of their employees, makes any warranty, express or implied, or assumes any legal liability or responsibility for the accuracy, completeness, or usefulness of any information, apparatus, product, or process disclosed, or represents that its use would not infringe privately owned rights. Reference herein to any specific commercial product, process, or service by trade name, trademark, manufacturer, or otherwise, does not necessarily constitute or imply its endorsement, recommendation, or favoring by the United States Government or any agency thereof. The views and opinions of authors expressed herein do not necessarily state or reflect those of the United States Government or any agency thereof.

D0 NOTE 2222
CDF/ELECTROWEAK/PHYS/PUBLIC/2758
August 29, 1994
FERMILAB-CONF-94/317-E

ELECTROWEAK PHYSICS FROM THE TEVATRON
Larry Nodulman
For proceedings of the Conference on Radiative
Corrections: Status and Outlook
Gatlinburg, TN
June 1994

ELECTROWEAK PHYSICS FROM THE TEVATRON

LARRY NODULMAN*

*HEP Division, Argonne National Lab.
Argonne, Illinois 60439, USA*

ABSTRACT

Results from the CDF and D0 detectors at the Fermilab Tevatron collider on electroweak physics are summarized. Topics include the top quark mass, the W boson width, trilinear couplings, and the W boson mass. Electroweak radiative corrections so far provide a consistent picture, and precision measurement constraints will continue to improve. The study of the top quark as well as diboson production is just getting started, and the W mass measurement will continue to improve.

1. Introduction

The main characteristics of production and detection of W and Z bosons at the Tevatron as well as the relevant characteristics of the CDF and D0 detectors will be summarized. The luminosity normalization for the two experiments will be compared. A concise summary of the top searches of the two experiments is followed by a discussion of the top mass implications. While CDF has a top mass measurement¹ of 174 ± 17 GeV/ c^2 , D0 has an lower limit of 131 GeV/ c^2 at 95% CL.² The two results are not contradictory.

Limits on W' and Z' production will be discussed as well as measurements of the W width. Trilinear couplings of $W\gamma$, $Z\gamma$, WW and WZ have been studied and so far are in agreement with expectations. Improved measurements with more statistics and combining the results of the two experiments will constitute a measurement of the W magnetic moment.

While electroweak radiative correction calculations make many measurements into the equivalent of being measurements of the mass of the W , both CDF and D0 have new direct measurements of the W mass of 80.38 ± 0.23 and 79.86 ± 0.35 GeV/ c^2 respectively, in good agreement with indirect and previous direct measurements.

2. Production and Detection of W s and Z s

Calculations of W and Z production in $\bar{p}p$ collisions continue to improve.³ Measurements of QCD characteristics of W and Z production are discussed elsewhere.⁴ At the Tevatron, leptonic signatures are required to identify W s and Z s, and for this discussion decays to τ only contribute as a correction to the e or μ spectra or as a source of background. The signature leptons (e or μ) have $p_T > 20$ GeV/ c and are not particularly associated with jets, thus usually isolated from other activity.

*Supported in part by the U. S. Department of Energy, Division of High Energy Physics, contract number W-31-109-ENG-38.

Both experiments associate a track with a characteristic electromagnetic shower in the calorimeter in order to identify electrons. In the central pseudorapidity region $|\eta| < 1.4$ CDF has a track momentum measurement in the magnetic field of the solenoid inside the calorimetry. Stiff tracks are matched to stubs in muon chambers outside the calorimeter to identify muons. D0 has more thorough muon coverage and the momentum measurement comes from magnetic deflection going through iron toroids.

The results being discussed are from data taken in 1992-3. The datasets of the two experiments coming from this run represent a major statistical improvement over what has been available previously. While the final UA2 dataset has less than 4000 electron W s⁵ and the 1988-9 CDF dataset less than 4000 W s in e and μ combined,⁶ the new data samples have 14000 electron and 7000 muon W s for CDF and 10000 electron and 1500 muon W s for D0. This substantial statistical improvement is reflected in many areas.

3. Luminosity Normalization

Both experiments use coincidence rates for scintillation counters along the beam-line on both sides (beam-beam counters) as a monitor of luminosity in the Tevatron. CDF performed a small angle spectrometer measurement of the luminosity independent total cross section⁷ which using only the ρ parameter from E710⁸ has been used to determine the CDF beam-beam counter cross section. This normalization was adopted recently¹ and represents approximately a 9% reduction in previously quoted luminosity (previous cross sections should be increased) with a considerable gain in accuracy, $\pm 7\%$ becomes $\pm < 4\%$. The normalization previously used by CDF was similar to the prescription used by D0. D0 extrapolates from UA4⁹ using the E710 total cross section.¹⁰ This method gives an accuracy for D0 of $\pm 12\%$. The D0 normalization is 9% higher than the old CDF normalization. The normalization definitions used for the measurements quoted here are different from each other by about 18%, as is reflected in the preliminary cross section times electron branching ratio for W s of $2.06 \pm 0.02 \pm 0.06 \pm 0.25$ nb for D0 and $2.51 \pm 0.02 \pm 0.07 \pm 0.10$ nb for CDF where the uncertainties are statistical, systematic and normalization. D0 has recently adopted a new normalization using the average of the E710 and CDF total cross sections. This update reduces the D0 integrated luminosity by 11%, greatly reducing the discrepancy between experiments; the new D0 cross section times branching ratio is $2.32 \pm 0.02 \pm 0.06 \pm 0.28$ nb.

Most data samples being discussed are from 20 pb^{-1} for CDF, new normalization, and 16 pb^{-1} for D0, old normalization.

4. The Top Quark

The dominant production mechanism for top quarks in $\bar{p}p$ collisions at 1.8 TeV is pair production of $\bar{t}t$. In the relevant mass range for top, each top quark decays into a real W and a b quark. Searches typically demand at least one W decay to e or μ giving a lepton and missing E_T . Further signature may be another isolated

Search Category	Expect m=160	Background	Observed
D0 SEARCHES			
Dilepton	0.83	0.98	1
Kinematic	2.8	1.6	3
Soft lepton tag	1.6	2.1	3
D0 SUM	5.4 ± 0.9	4.7 ± 1.0	7
CDF SEARCHES			
Dilepton	1.3	0.56	2
Soft lepton tag	1.9	3.1	7
Silicon vertex tag	2.7	2.3	6
CDF SUM	5.9	5.9	15 (12 events)

Table 1: D0 and CDF Top Searches at a Glance

e or μ (dilepton), a tag of a jet as being a b by means of an associated e or μ (soft lepton tag), by flight path (Silicon vertex tag) or by the kinematics of the jets (kinematics). In each case a minimal presence of jets is required to make the event plausible as top and to reduce the W plus jets, standard model W pair and τ pair backgrounds. The preliminary updated D0 search² and the published CDF search¹ are summarized in Table 1. Expectations are for the NNLO cross section¹¹ for a top mass of 160 GeV/c² as normalized by each experiment. In addition, CDF has done a kinematic search finding 14 events with a background of about five which is not included in the table.¹²

The D0 group uses the predicted cross section as a function of mass and the small number of events to set a lower limit on the top mass of 131 GeV/c² at the 95% CL.² The D0 observation is not significantly in excess of the background expectation. The excess number of tags in the CDF tabulated searches is of modest statistical significance. The probability of background fluctuation is 0.28% based on tag counting. Top-like kinematics of the events and b tags in the dilepton events are not contributors to the quoted probability. CDF determines a top mass from the kinematics of the lepton plus tag events. The results from the two experiments are not incompatible as can be seen in Fig. 1.

CDF uses the SQUAW fitting program to fit a lepton plus tag event to the $\bar{t}t$ hypothesis. There must be four jets in an event to assign to the two W decay jets and the two b jets. Seven of the ten lepton plus jet events satisfy appropriate jet requirements. With the W mass constraint and the constraint that the two tops be of equal mass, the kinematics is overconstrained by 2. Both neutrino solutions are used. The jet tagged to be a b is assigned only as a b . The four highest E_T jets are used and the solution with the lowest χ^2 is used as long as $m(\text{top}) < 260$ GeV/c². The mass spectrum expected for 170 GeV/c² is illustrated in Fig. 2a; wrong combinations widen the distribution but do not completely spoil the measurement. The fit of the data to background plus top is shown in Fig. 2b. The fit prefers top

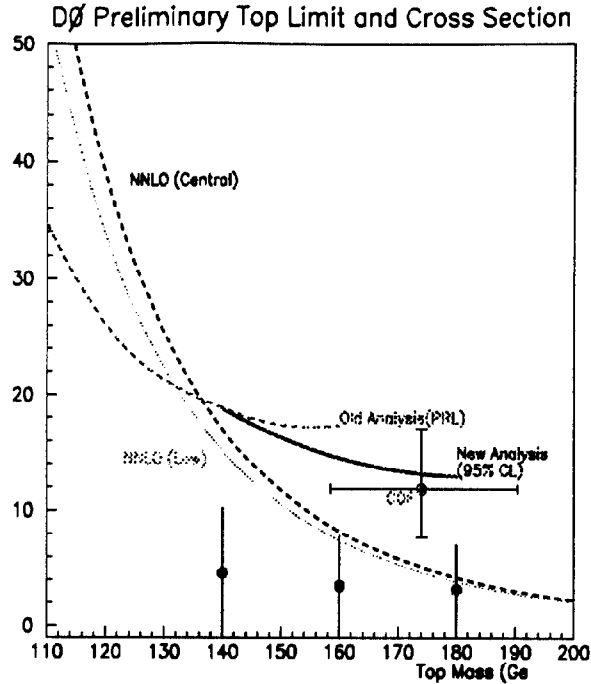


Figure 1: Cross section for top pair production (pbarn) from the D0 search, updated since the limit publication, showing the CDF measurement scaled to the D0 normalization, and the NNLO prediction both nominal and lowest.

to no top by a factor of 50 in probability. The top mass has a statistical uncertainty of ± 10 GeV/c². Systematic uncertainties are +5.3 – 4.4% for background shape, $\pm 4.4\%$ for gluon radiation effects, $\pm 1.8\%$ for calorimeter energy scale (helped by the W mass constraint), $\pm 1.4\%$ for jet energy bias due to tagging and $\pm 1.1\%$ to cover variation with different fitting programs and procedures. So the top mass obtained is $174 \pm 10_{-12}^{+13}$ GeV/c². This is to be compared with top masses inferred from LEP data, neutrino neutral currents, SLD, and W mass measurements which range from 162 to 177 depending on which data is included, with statistical uncertainties of as low as ± 12 depending also on willingness to combine contradictory measurements. The variation with Higgs mass is about ± 18 GeV/c².¹³

5. The W' and Z' Searches

Various models which are extensions of the standard model predict heavier charged and neutral vector bosons. While the couplings of such bosons depend on the details of the model, limits quoted on the production of such particles, for definiteness, are for standard model equivalent coupling. For a W' , fits are done attempting to add an additional Jacobean peak to the transverse mass spectra. This is illustrated by the D0 W' preliminary search shown in Fig. 3. D0 rules out such a W' with mass less than 620 GeV/c² at 95% CL. Similarly, again preliminary and for electrons, CDF excludes W' mass below 652 GeV/c². Presumably a higher limit could be obtained combining the results.

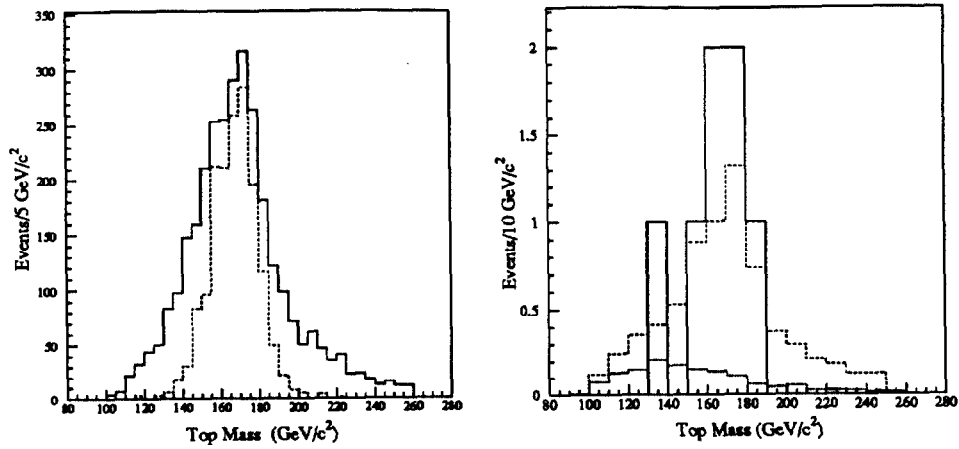


Figure 2: Top mass spectra (left) for a Monte Carlo top mass of $170 \text{ GeV}/c^2$ where the dashed histogram shows the peak for those cases (about one third) when the correct jet assignments happen to be made, and (right) for the seven CDF data events where the dashed histogram shows the fit and the background, as fit, is the dotted histogram.

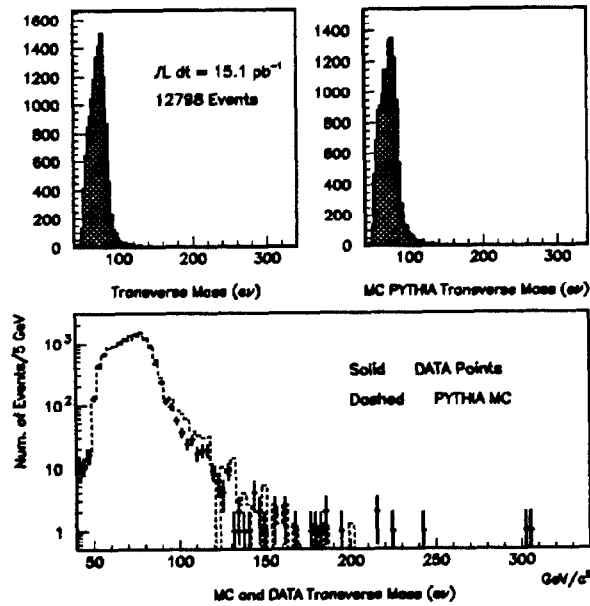


Figure 3: D0 W transverse mass tail compared to Monte Carlo predictions to set a preliminary limit on W' production, on linear and log scales.

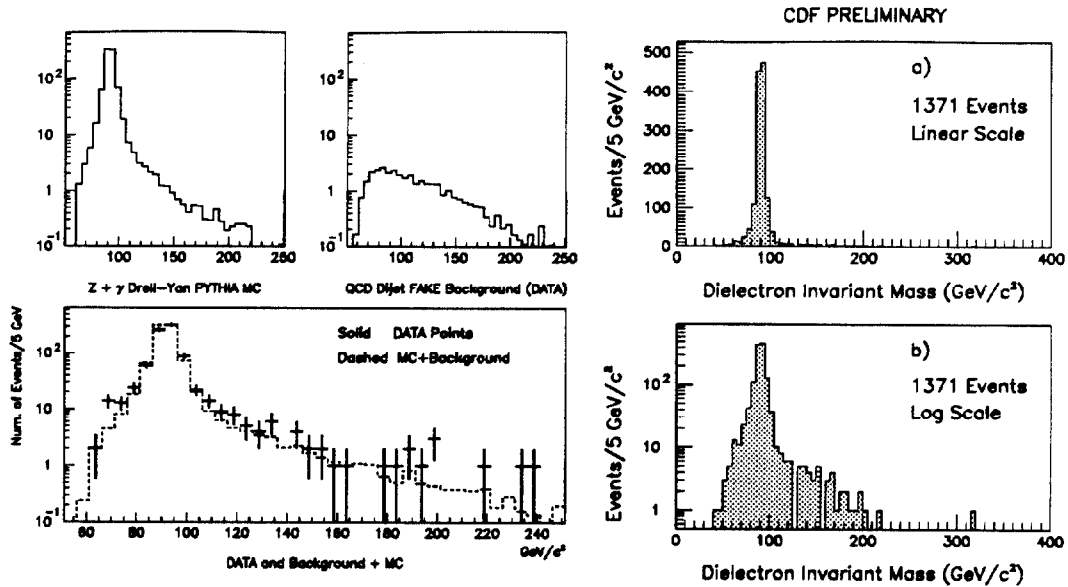


Figure 4: Preliminary dielectron mass spectra for the Z' search. The D0 spectra (left) for signal and background predictions are above. The histogram below is the Z plus background prediction, shown with the data points. There are 886 data events. The CDF spectrum (right), linear and log, is also for 92/93 data.

The Z' searches involve invariant mass with Drell Yan continuum as well as the Z in the standard prediction. The 92/93 electron data for D0 and CDF are shown in Fig. 4. For standard model equivalent couplings, limits of 480 and 505 GeV/c^2 are obtained from the respective collaborations. In the new 94 data CDF has an electron pair candidate event with a mass of 510 GeV/c^2 , not quite exciting.

6. The W Width

As with the Z width, if the W width agrees very well with the expectation based on predicted decay modes, other decay possibilities can be excluded. These possibilities in W decay are not as interesting as say further flavors of light neutrinos. Historically, W decay to $t\bar{b}$ where the top could then decay to anything, for example to H^+b , and thus not be seen in direct collider top searches, would be noticed in the W width. Top by definition is the isospin partner of bottom and the kinematical suppression afforded by a top mass of at least 62 GeV/c^2 can be inferred at 95% CL.¹⁴ The usual way to infer the width of the W is from the ratio of cross section times say electron branching ratio for W and Z . The ratio of cross sections is taken from QCD calculation¹⁵ and each branching ratio is the ratio of the partial width to the total width. The Z numbers are well measured at LEP and the W leptonic partial width is readily obtained from the muon mass and lifetime and

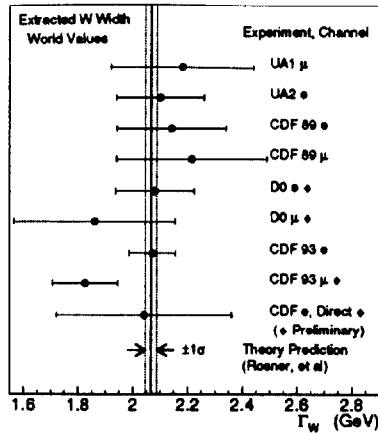


Figure 5: Summary of indirect and direct measurements of the W width.

the W mass, leaving the W total width to be determined. CDF has obtained a W width of $2.06 \pm 0.06 \pm 0.06$ GeV for electron decays¹⁴ with a preliminary muon result of $1.83 \pm 0.09 \pm 0.08$ GeV. D0 has preliminary values of $2.08 \pm 0.08 \pm 0.12$ GeV for electron decays and $1.86 \pm 0.24 \pm 0.17$ GeV for muon modes. CDF also has a preliminary direct measurement using the Breit Wigner tail of the W in transverse mass far beyond resolution smearing for the bulk of the events. The 58 electron events with transverse mass above $110 \text{ GeV}/c^2$ correspond to a W width of $2.04 \pm 0.28 \pm 0.16$ GeV. These measurements are summarized in Fig. 5 and compare well to a standard model prediction of 2.07 ± 0.02 GeV.¹⁶

7. Trilinear Couplings

The couplings among the W , Z and γ are determined in the standard model in order to give the unitarity preserving destructive interference which the standard model was invented to provide. Nonstandard couplings could arise if one or more of the bosons was composite.

The study of events with a photon produced along with a W should show the interference of photon coupling to the final state e or μ from the W , coupling to initial state quarks and coupling to the W itself. Of the several possible coupling parameters,¹⁷ the most commonly studied are the CP conserving couplings κ and λ where the W magnetic dipole moment is given by $e/(2 m(W))$ times $(1 + \kappa + \lambda)$ and the electric quadrupole moment is similarly proportional to $(\kappa - \lambda)$. Since the standard model values are 1 for κ and 0 for λ , nonstandard searches look at λ and $\Delta\kappa$ which is of course defined as $\kappa - 1$.

Both experiments use the shape of the photon E_T spectrum to derive coupling limits. These spectra are shown in Fig. 6 and limits are shown in Fig. 7 compared to previous results.¹⁸ The contours for the two experiments are quite similar and since both results are predominantly statistically limited, a combined limit should reduce the ellipse axes by nearly 30%. The CDF contour, for example, represents a

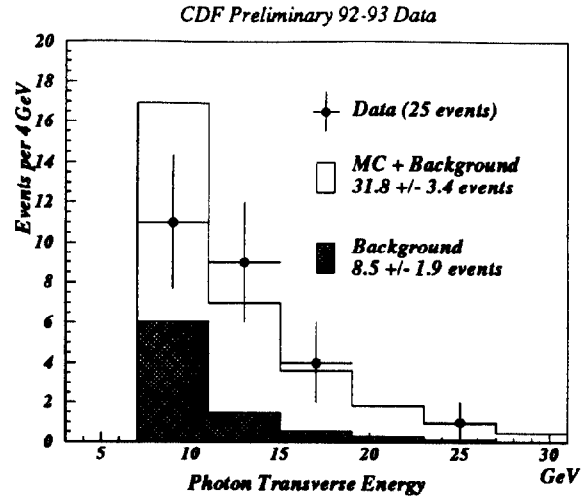
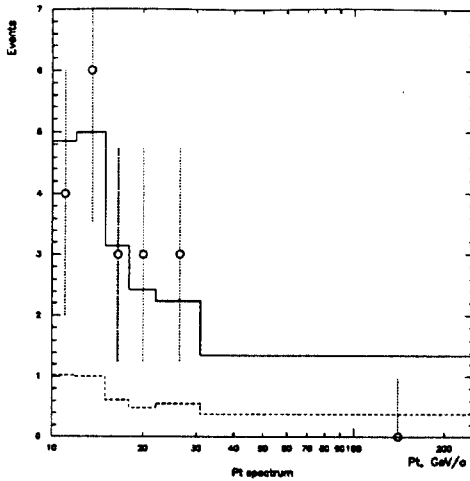


Figure 6: E_T spectra for photons in $W\gamma$ events for D0 (left) and CDF (right). In both cases the points are the observed events, the upper histogram is the sum of signal and background expectation, and the lower histogram is background.

measurement of the scaled W magnetic moment g_W , supposed to be 2, of 2.0 ± 0.7 .

CDF has derived coupling limits from 8 $Z\gamma$ events observed with 7.1 signal and 0.5 background events expected. For example the restrictions $-2.9 < h_{30}^Z < 3.0$, $-3.1 < h_{30}^\gamma < 3.1$, $-0.7 < h_{40}^Z < 0.7$, and $-0.8 < h_{40}^\gamma < 0.8$ are for 95% CL.

Similar considerations apply to WW and WZ production. D0 has set relatively weak coupling limits looking at all leptonic decays. CDF, while observing one spectacular three electron WZ event, sets better limits by using the $lvjetjet$ and $lljetjet$ modes and taking advantage of the relatively prolific high E_T production characteristic of nonstandard couplings. Jet pair mass is required to be consistent with coming from a W or Z and the p_T of the W or Z jet pair is required to be above 130 GeV/c if opposite a leptonic W and above 100 GeV/c if opposite a leptonic Z . These cuts were designed to essentially remove W and Z plus jets background. One W jet jet and no Z jet jet events are found. Note that in this high p_T regime, whatever effect (form factor) eventually restores unitarity will restrict the range of coupling which could be observed and dilute the limits derived. Fig. 8 shows limits for a sampling of combinations of couplings, and some limits obtained in combination with the $W\gamma$ data.

8. The W Mass

Both experiments restrict themselves to high p_T clean central samples for this measurement. Lepton p_T and missing E_T are required to be above 25 GeV/c and leptons are restricted to pseudorapidity $|\eta| < 1$. Clean events are selected by, for example, asking that the p_T of the W be less than 30 GeV/c.

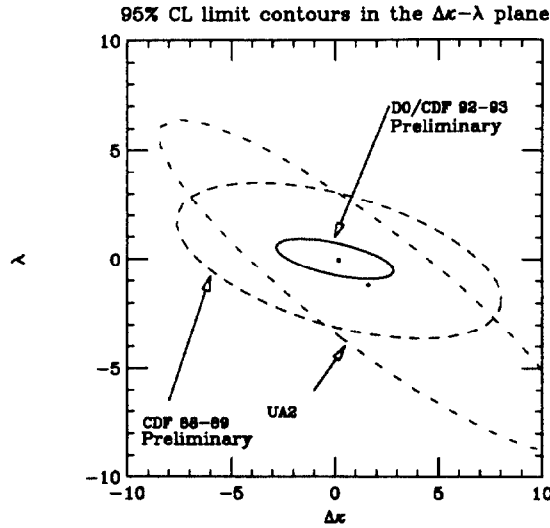


Figure 7: Coupling limit contours in the $\Delta\kappa - \lambda$ plane. The solid and dotted contours which are indistinguishable as they are essentially the same, are from D0 and CDF.

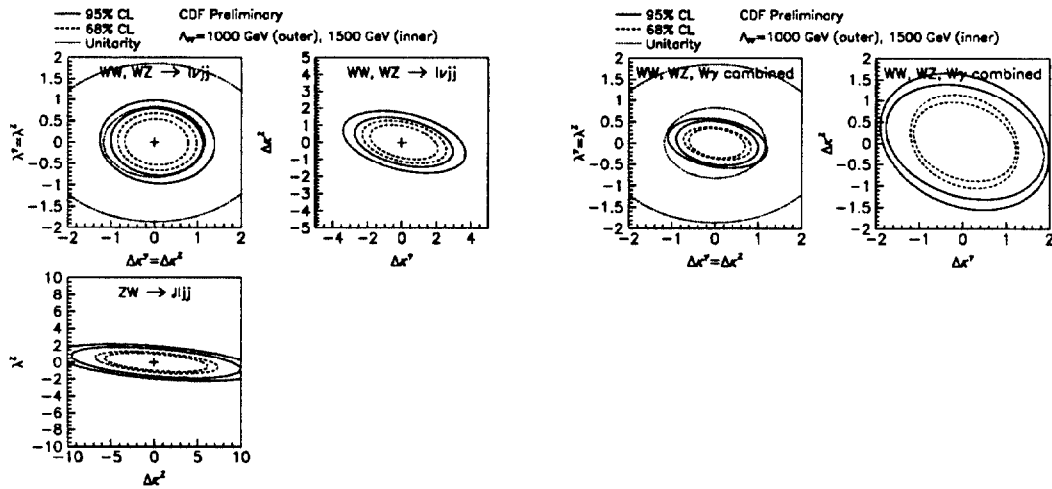


Figure 8: CDF preliminary limit contours for diboson couplings from the WW and WZ search (left). The upper left assumes λ and κ are the same for γ and Z , the others do not. In all cases the dilution from form factor effects is illustrated by plotting limits for cutoff parameter Λ_{FF} both 1000 and 1500 (inner ellipses) GeV. CDF preliminary limit contours for WW , WZ and $W\gamma$ data combined (right) sample the many possibilities.

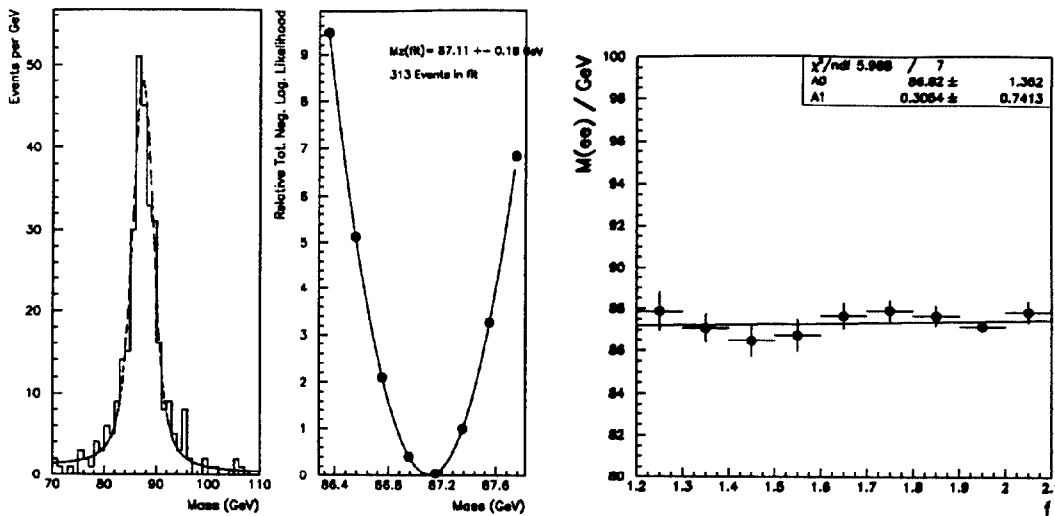


Figure 9: D0 unscaled Z mass (left), the fit to it (middle) and slope (f) constraint from Z electrons (right).

Transverse mass is defined by $m_T^2 = 2p_{Tl}p_{T\nu}(1 - \cos(\Delta\phi))$. The neutrino ($p_{T\nu}$) is reconstructed as the reverse of both the lepton (p_{Tl}) plus the recoil to the W p_T . The recoil is reconstructed from the calorimeter and denoted u . For small W p_T , m_T is approximately $2p_{Tl} + u_{||}$ where $u_{||}$ is the suitably signed projection of u onto the lepton azimuth. D0 uses the range $60 < m_T < 90$ and has 5830 electron events. CDF uses $60 < m_T < 100$ and has 6508 electron events and 4090 muon events.

A prime experimental concern is to establish the lepton energy/momentum scale. D0 uses the Z mass; the observed value of 87.11 ± 0.18 GeV/c^2 is scaled to the LEP value. Possible nonlinearity is constrained by defining a slope reflecting the energy variation of the electrons within the Z sample. These are shown in Fig. 9; the linearity slope parameter f is defined by $f = 2(E_1 + E_2)/m \sin(\gamma)$ where the energies and mass are as observed and γ is the opening angle. This procedure leaves an uncertainty in the energy scale corresponding to ± 260 MeV/c^2 . It is hoped that constraints from the ψ dielectron and the π^0 masses will help to constrain the slope and reduce this uncertainty.

CDF uses the ψ dimuon mass to calibrate the magnetic tracking system. Constraining the ψ mass to the PDG value results in a momentum scale factor of 1.00076 ± 0.00071 which is confirmed by checking the Υ s and the Z . The ψ and the Υ s are shown in Fig. 10. For electrons, the tracking calibration is transferred to the calorimeter using E/p along with a radiative simulation as shown in Fig. 11. The radiative tail determines the amount of material to put into the simulation, as well as into a dE/dx correction for the muons above. The peak position is used to determine the calorimeter energy scale. Muon momentum scale is accurate to ± 60 MeV/c^2 at the W and the E/p match and particularly the material determination raise the scale uncertainty to ± 130 MeV/c^2 for electrons.

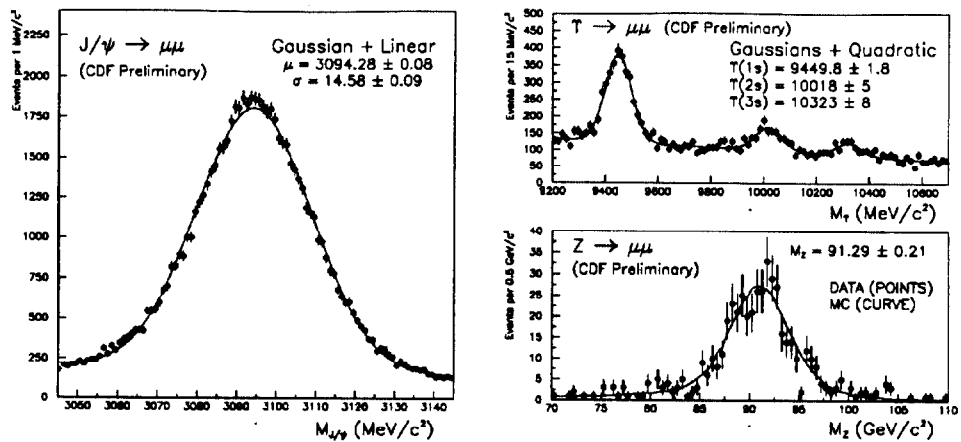


Figure 10: The CDF dimuon ψ mass (left), used to calibrate the tracking scale and the Υ masses and $Z \rightarrow \mu\mu$ mass (right), used as checks.

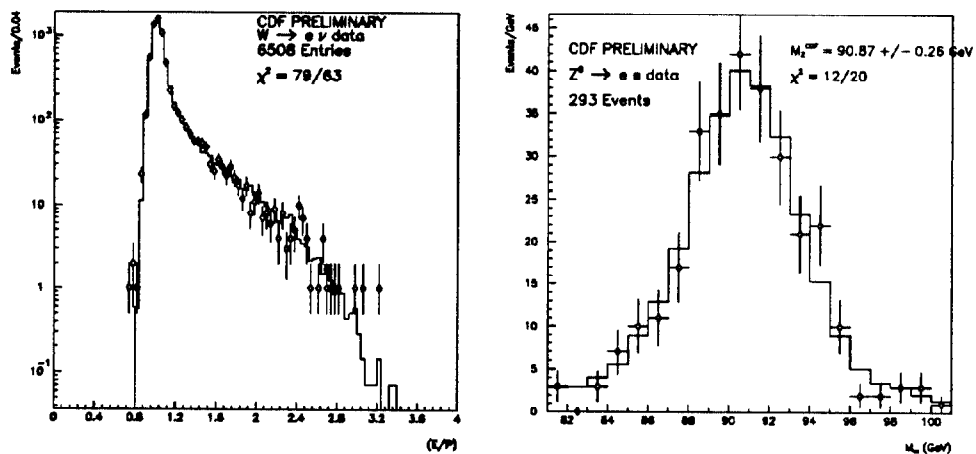


Figure 11: CDF E/p distribution for W mass candidates and the radiative simulation (left) and the $Z \rightarrow ee$ mass, used as a check (right).

	D0	CDF		
	electron	electron	common	muon
Statistics	160	150		200
Scale	260	130	60	60
Systematics	160	190	130	190
lepton resolution	70	140		120
$u_{ }$	50	70		90
recoil and event	95		90	
p_T input	50	40		70
theory (PDFs)	70		100	
background	30	50		50
fitting	30	20		20

Table 2: D0 and CDF preliminary W mass uncertainties in MeV/c^2 . Those uncertainties which are common to both the e and μ analyses in CDF are listed separately.

Both experiments use fast Monte Carlo simulations of W production and detector response to predict the transverse mass spectrum as a function of W mass. Key concerns are understanding the resolution in lepton p_T measurement, understanding any bias in the recoil measurement in the lepton direction ($u_{||}$), the calorimeter response to the recoil including the background event, the W p_T spectrum generated, the production theory uncertainties particularly PDF's, the bias due to background contamination, and the systematics associated with fitting. D0 uses a recoil response model which is constrained by the Z data and uses minimum bias events for the background event. CDF uses the background event and recoil of Z events directly, picking Z events with appropriate p_T of the W matching p_T of the Z as measured by the leptons. The W mass uncertainties are summarized in Table 2.

A notable detail is that the D0 analysis has not yet applied radiative corrections for wide angle photons either to the Z mass used for scale or for the W mass. Preliminary CDF radiative corrections are 80 and 154 MeV/c^2 for the electron and muon W masses, and 140 and 310 MeV/c^2 for the Z masses. All shifts go up. The difference between electrons and muons comes from colinear photons.

The transverse mass fits are shown in Fig. 12. The D0 preliminary result is $79.86 \pm 0.16 \pm 0.16 \pm 0.26 \text{ GeV}/c^2$. The CDF preliminary results are $80.47 \pm 0.15 \pm 0.19 \pm 0.13 \text{ GeV}/c^2$ for electrons and $80.29 \pm 0.20 \pm 0.19 \pm 0.06 \text{ GeV}/c^2$ for muons which combine to $80.38 \pm 0.23 \text{ GeV}/c^2$. These agree well with previous measurements by UA2⁵ and CDF¹⁹ and the four can be combined to $80.23 \pm 0.18 \text{ GeV}/c^2$ where 100 MeV/c^2 has been conservatively assumed to be globally common uncertainty in hadron collider measurement. These results agree with indirect inference from LEP data¹³ and neutrino neutral current measurements²⁰ but not the A_{LR} measurement at SLD.²¹

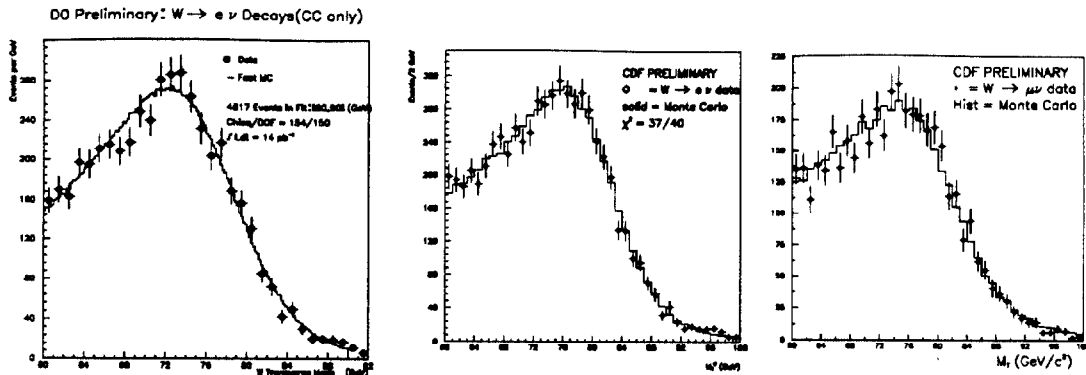


Figure 12: W transverse mass distributions for D0 electron events (left), CDF electron events (middle) and CDF muon events (right). Note that D0 plots from 60 to 92 and CDF plots from 60 to 100 GeV/c².

9. Conclusions and Outlook

A general conclusion on precision electroweak measurements is that there is no strong need for physics beyond the standard model. No significant constraint on the Higgs mass is yet obtained. There is no sign of further vector bosons, couplings seem well behaved, and there is not much room left for nonstandard W decay. This trend of predictability is illustrated in Fig. 13 where the LEP Z mass and Higgs mass assumptions are used in electroweak radiative correction calculations to relate the top and W masses.²² Note that including indirect W mass measurements would narrow that band substantially, but that even with substantial improvement there and say a factor 3 improvement on the top mass, the Higgs mass constraint may not be all that strong. At least the top mass has become the output of kinematic fits to events and not just fits to precision electroweak measurements.

Many of the preliminary analyses of 92/93 data quoted here should be completed soon. Another, even longer collider running period for the Tevatron got under way at the end of 1993. It is scheduled to continue till at least the fall of 1995. Although it got off to a rather slow start, the recent performance of the Tevatron, with luminosities of in excess of $1.5 \cdot 10^{31} \text{ cm}^{-2} \text{ sec}^{-1}$ make predictions of dataset of 150 pb^{-1} per experiment seem quite credible. This run will be followed by a several year long collider shutdown for fixed target running, installation of the main injector and collider detector upgrades including the D0 solenoid. Further collider running, with additional proton and antiproton bunches, should produce samples of 500-1000 pb^{-1} per experiment.

Both top mass measurements and diboson production studies will readily advance beyond their current relatively primitive statistical state. The numbers of $\bar{t}t$, $W\gamma$, $Z\gamma$, WW and WZ candidates need to rise substantially to permit improved analysis. Some of these measurements will remain clearly interesting even once LEP2 approaches its designed accuracy.

Progress in improving the W mass measurement will be less straightforward.

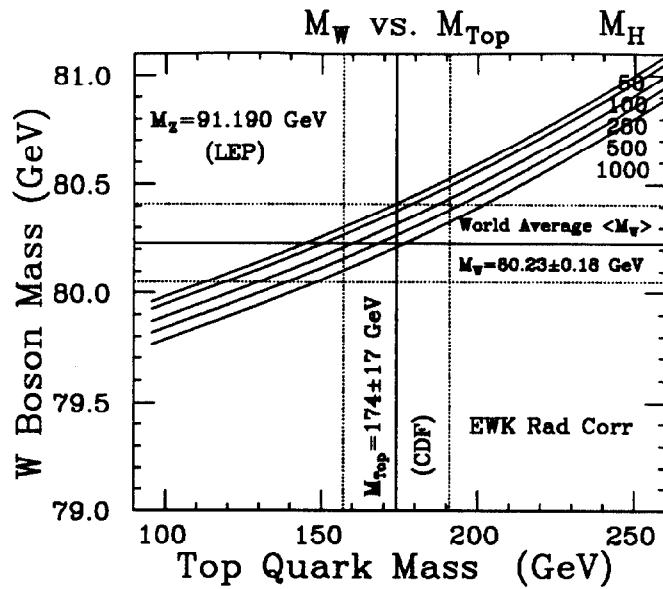


Figure 13: Top mass versus W mass.

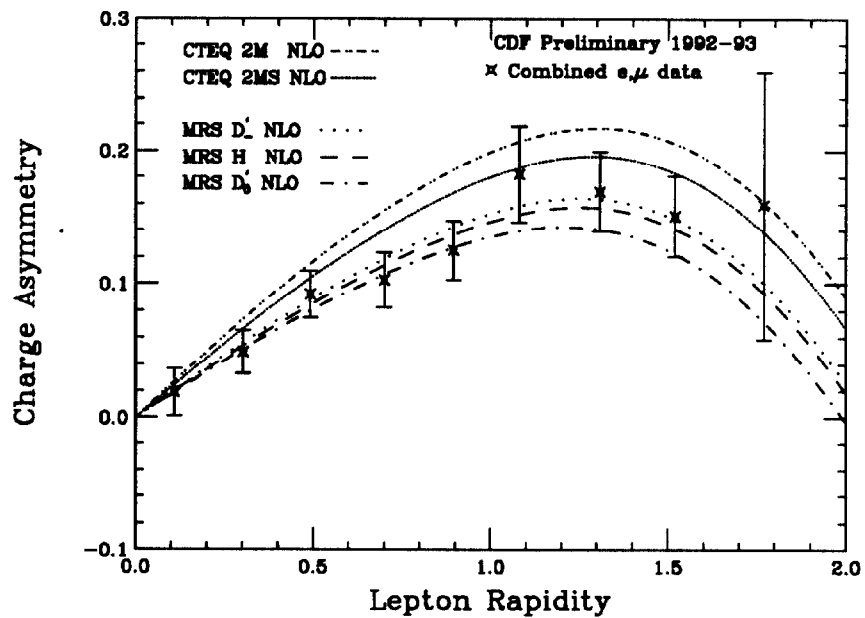


Figure 14: Lepton charge asymmetry from W decay versus pseudorapidity.

Improvement is expected although the difficulty of the measurement will increase. Many of the systematic effects are studied using various data samples, most usually Z events. The W data itself can be used to constrain even the theoretical uncertainty, as illustrated by the W charge asymmetry measurement²³ which will decrease the W mass variation with PDFs by favorably narrowing the range of viable PDFs as shown in Fig. 14. Clearly LEP2 should provide a challenge to this program.

10. Acknowledgements

I would like to thank the members of the D0 and CDF collaborations who have been most cooperative. In particular I would like to thank Marcel Demarteau, Paul Derwent and Young Kee Kim.

11. References

1. F. Abe *et al.* (CDF), *subm. Phys. Rev.*, FERMILAB-PUB-94/097-E.
2. S. Abachi *et al.* (D0), *Phys. Rev. Lett.* **72**, 2138 (1994); update as per M. Narain, Fermilab Users Meeting, June 1994.
3. See eg. A. D. Martin *et al.*, Rutherford Appleton Lab. Preprint RAL-94-055 (1994), W. Giele *et al.*, FERMILAB-PUB-92/230-T.
4. S. Linn, these proceedings.
5. J. Alitti *et al.* (UA2), *Phys. Lett.* **B276**, 354 (1992).
6. F. Abe *et al.* (CDF), *Phys. Rev D***44**, 91 (1991).
7. F. Abe *et al.* (CDF), *subm. Phys. Rev.*, FERMILAB-PUB-93/232-E, FERMILAB-PUB-93/233-E and FERMILAB-PUB-93/234-E.
8. N. A. Amos *et al.* (E710), *Phys. Rev. Lett.* **68**, 2433 (1992).
9. M. Bozzo *et al.* (UA4), *Phys. Lett.* **B147**, 392 (1984).
10. N. A. Amos *et al.* (E710), *Phys. Lett.* **B243**, 158 (1990).
11. E. Laenen *et al.*, *Phys. Lett.* **321B**, 254 (1994).
12. See eg. F. Abe *et al.* (CDF), FERMILAB-CONF-94/152-E (Glasgow).
13. A. Blondel, these proceedings.
14. F. Abe *et al.* (CDF), *Phys. Rev. Lett.* **73**, 220 (1994).
15. A. D. Martin *et al.*, *Phys. Lett.* **228B**, 149 (1989) and W. J. Stirling, private communication
16. J. Rosner *et al.*, Enrico Fermi Institute preprint EFI-93-40 (1993).
17. K. Hagiwara *et al.*, *Phys. Rev. D***41**, 2113 (1990).
18. J. Alitti *et al.* (UA2), *Phys. Lett.* **B277**, 194 (1992).
19. F. Abe *et al.* (CDF), *Phys. Rev. D***43**, 2070 (1991).
20. T. Bolton, these proceedings.
21. P. Rowson, these proceedings.
22. F. Halzen and B. A. Kniehl, *Nucl. Phys.* **B353**, 567 (1991).
23. F. Abe *et al.* (CDF), FERMILAB-CONF-94/146-E (Glasgow).